FINITE ELEMENT MODELING OF SELF-COMPACTING CONCRETE BEAMS UNDER SHEAR

Elham HOSSEINIMEHRAB[1], Abbasali SADEGHI[2],
Ehsan NOROOZINEJAD FARSANGI[3,4]
[1] Department of Civil Engineering, Vahdat Institute of Higher Education, Torbat-e Jam, Iran
[2] Department of Civil Engineering, Islamic Azad University, Mashhad Branch, Mashhad, Iran
[3] Faculty of Civil and Surveying Engineering, Graduate University of Advanced Technology, Kerman, Iran
[4] School of Civil Engineering and the Built Environment, University of Johannesburg, Johannesburg, South Africa

A b s t r a c t

Development of self-compacting concrete (SCC) is a very desirable achievement in the reinforced concrete (RC) structures for overcoming issues associated with many problems such as congestions of steel reinforcement. This non-vibrating concrete is not affected by the skill of workers, and the shape and amount of reinforcing bar arrangement of a structure. Due to the high fluidity and resisting power of reinforcing of SCC, it can be pumped longer distances. In this study, the finite element (FE) modeling of three SCC beams in shear while taking into account, the flexural tensile strength of concrete is computed and the results are compared with the available experimental tested reinforced SCC beams. The stirrups are located at 75 mm apart from the end of beams up to the loading point. The electrical strain gauges (ESGs) have been embedded on the stirrups and their strain readings are taken for every step of load increment. For modeling longitudinal steel reinforcing bars and concrete, the 3-D elements with 2-node and 8-node, are used

Corresponding author: Assistant Professor, Faculty of Civil and Surveying Engineering, Graduate University of Advanced Technology, P.O. Box 117-76315, Kerman 7631818356, Iran. Email: noroozinejad@kgut.ac.ir

respectively. The comparison of results obtained by two methods is indicated that a good satisfactory agreement is achieved.

Keywords: Self-compacting concrete (SCC), shear capacity, finite element (FE) modeling, electrical strain gauges (ESGs)

1.   INTRODUCTION

Because of its adaptability in taking on any structural shape, concrete has proven to be a highly effective construction material for building buildings. Steel reinforcements in concrete instantly changed the building industry, defining new boundaries and pushing reinforced concrete - as it became called - to its structural limits. Researchers and practitioners have recently created a new form of concrete material known as self-compacting concrete (SCC). This form of concrete may flow under its own weight without requiring vibration. As a result, it is arguably more cost-effective and long-lasting. One way to reduce the intensive labour demand for vibration of highly congested reinforced sections is to use the new generation type of concrete called as SCC which is developed in Japan by Okamura in the late 1980s in order to reach durable concrete structures [1]. Since that time, Japanese contractors have used SCC in different applications. In contrast with Japan, research in Europe, US, and Iran started only recently [2-4]. Such concrete can spread readily into place and fill the formwork without any mechanical consolidation and with minimum risk of separation of the material constituents.

Researchers set out to explore the mechanical characteristics and structural reactions of this new type of concrete using various techniques in order to better understand its properties. In the following, the background of the study is presented.

To better understand the unreinforced behavior of SCC under shear, Hossain et al. (2008) investigated the shear strength of SCC beams with no shear reinforcement. The results showed that the ultimate shear strength of SCC beams is lower than that of normal concrete (NC) beams, and that this difference may be more evident in specimens with less longitudinal steel reinforcement and greater beam depth [5]. Fritih et al. (2013) evaluated the influence of steel fiber reinforcement on the behavior of SCC beams. Bending experiments were performed to investigate the influence of low fiber content (0.25 percent by volume) on the flexural behavior of beams reinforced with various quantities of steel rebar. The investigation examined the behavior of reinforced concrete beams cast using either control SCC or fiber-reinforced self-compacting concrete (FRSCC). The findings indicated that fiber reinforcing improves cracking control. The fiber reinforcement has little influence on yielding, ductility, or load-bearing capability; its effects are restricted

to crack kinetics and dispersion [6]. Ahmad et al. (2016) tried to compare the characteristics of SCC to those of normal concrete (NC). They looked at the compressive and splitting tensile strengths of three concrete mixes: NC, SCC, and SCC reinforced with fiber glass. SCC's compressive and splitting tensile strengths were found to be somewhat greater than those of the equivalent NC specimen [7]. Lif et al. (2016) examined the mechanical characteristics of concrete using various percentages of basalt, polypropylene, and glass fiber, such as 0.5 percent, 1.0 percent, 1.5 percent, 2.0 percent, and 2.5 percent. The results reveal that basalt, polypropylene, and glass fiber have a substantial effect on the modulus of elasticity, as well as compressive and flexural strength [8]. Tahir (2018) investigated the material, mechanical, and structural characteristics of SCC reinforced with 0.5 and 1% coir fiber. The results showed that 0.5 percent coir fiber in SCC increased compressive, tensile, and flexural strength. The mechanical characteristics of coir fiber were added to SCC based on prior research. As a result, the use of coir fiber in SCC will minimize solid waste while also addressing corrosion issues caused by the use of steel in SCC [9]. ABAQUS finite element (FE) modeling tool was used to investigate the structural behavior of the reinforced SCC deep beam by Akinpelu and Adedeji (2018). The mentioned study found that doubling the concrete compressive strength resulted in 41.1%and 49% increases in diagonal cracking and ultimate load, respectively, in the specimens [10]. Beam torsional behaviours are examined for web reinforcement and concrete type by Aydin and Bayrak (2019). Eight SCC beams and twelve conventional concrete (CC) beams were built and tested. All units manufactured as the 250x300x1500 mm were tested in accordance with applicable requirements. Two concrete kinds, CC and SCC, were developed with compressive strengths of 20 and 40 MPa, respectively. The web spacing was set at 80 and 100 mm from the site of web reinforcement. The ultimate and critical torsional moments, as well as the rotation angles of the concrete beams exposed to pure torsional force, were measured [11]. Akinpelu et al. (2019) checked the experimental and analytical connections that exist between the splitting tensile strength and compressive strength of identical grades of vibrated concrete (VC) and SCC. The experimental results revealed that the splitting tensile to compressive strength ratio for VC and SCC decreases with increasing compressive strength, and the analytical study revealed that a similar analytical model could be used for both concrete types because there is no statistically detectable difference between their results [12]. Jain et al. (2020) used granite waste (GW) and fly ash as fine aggregate and cement alternatives, respectively, for the sustainable production of SCC. Slump flow, T500 flow, V-funnel, J-ring, and L-box tests were used to evaluate fresh properties, while compressive strength, flexural strength, water absorption, and ultrasonic pulse velocity tests were used to evaluate hardened properties. The

results of the fresh properties revealed that the incorporation of GW had a negative impact on them. However, the incorporation of fly ash improved the fresh properties and mitigated the negative effect of GW on the fresh properties to some extent. [13]. Hussein et al. (2021) present the results of an experimental and numerical study of the behavior of reinforced concrete hybrid beams under two-point load. Eight beams (1502001300 mm) in length were cast and tested. The hybrid specimens are composed of two layers, the upper layer (in the compression zone) of SCC with a compressive strength of approximately 75 MPa and the lower layer (in the tension zone) of normal strength concrete (NSC) with a compressive strength of approximately 30 MPa. The results of the tests revealed that utilizing hybrid concrete in the casting of reinforced beams had a substantial influence on improving the overall behavior of the specimens [14].

One of the barriers to the widespread acceptance of SCC is the limited information regarding structural properties of sections cast with SCC, especially while considering the shear capacity of the elements either numerically or experimentally. The main objective of the study reported herein was to compare the experimental results of the shear performance of reinforced SCC beams to that of the FE modeling [15] while taking into account the flexural tensile strength of concrete f_r. The comparison of the results by two methods is indicated that, a good coincidence is available. However, in the experimental phase, the results obtained of three reinforced SCC beams tested by the first author are used. It has remained that the behavior of tested beams with SCC under flexure is reported by valid research [16]. The SCC beams are theoretically designed for shear based on the provision of ACI-08 [17] for conventionally vibrated concrete. There is no standard to design the reinforced SCC structures, and therefore the ACI Code validity in shear is as well confirmed.

2. MATERIALS

The approach in this research on the development of SCC for casting reinforced beams involved using high paste volume (and low aggregate volume) to promote high deformability and reduce the risk of blockage and segregation during concrete placement. SCC can be distinguished from conventional concrete not only by its high fluidity but also by its composition. The most important distinctions are:

1- Using a high content of powder materials (<80 μm, from 450 to 600 kg/m3) that necessitates the replacement of up to 50% of the powder content by supplementary cementations materials and/or fillers.

2- Use of large quantities of superplasticizer and use of a viscosity-enhancing admixture in some cases when the water content is not low enough to promote sufficient viscosity of the paste.

3.   EXPERIMENTAL PROGRAM

Three simply supported reinforced SCC beams (SCCB1-SCCB3) with 300*200 dimension and 3000 mm length were tested under two-point loading (statistical increasing) with a constant moment region (Fig. 1). All beams were designed for the shear span to depth ratio of 3.5. The clear cover for the tested beams was maintained at a minimum of 25 mm. For each mix, three numbers of 100 mm cubes for compressive strength were tested; the beams and the companion concrete specimens were demoulded after 24 h and were cured with wet hessian (spraying the water twice a day, similar to site curing) for 6 days. After that, the specimens were air-cured with a relative humidity of 65–80% and ambient temperature 28±3 ºC until the age of testing.

(a)   Details of tested beams
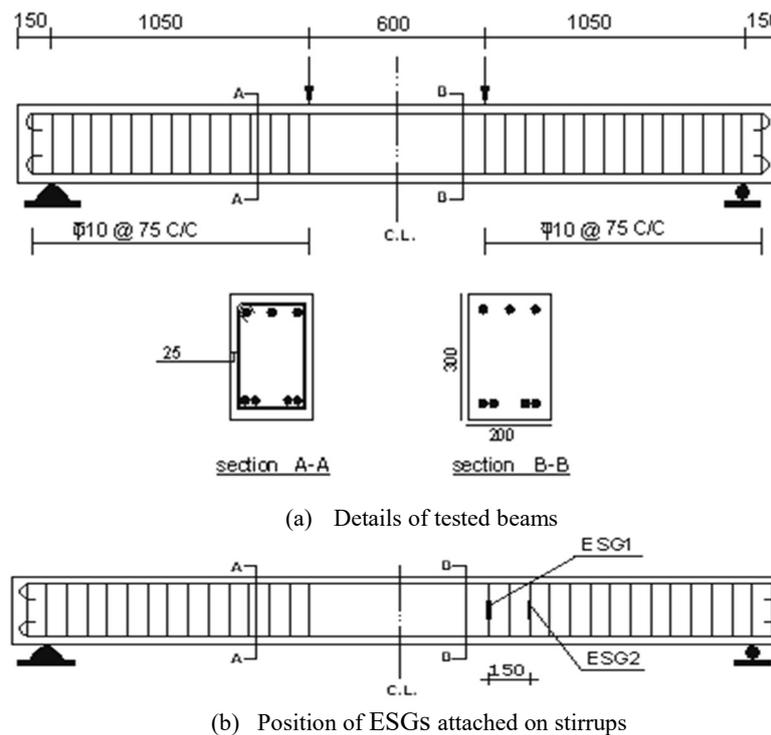

(b)   Position of ESGs attached on stirrups
Fig. 1. Details of test beams and position of ESGs on stirrups

The load was applied statically in 20 to 25 increments up to failure using a 1400 kN testing machine. The beams were instrumented with linear voltage displacement transducers (LVDT) to monitor deflection. Mechanical strain gauges (demec) were used to measure the surface concrete strain at different locations, and the steel strains were measured by the electrical strain gauges (ESGs) attached to the stirrups at different positions. During the test, the strains and deformation readings were recorded mechanically or automatically using a data logger. The beams' details are presented in Table 1. The typical test set for the tested beams is shown in Fig. 2.

Table 1. Details of the experimental program of tested beams

Beam No.	f'$_c$ (MPa)	d (mm)	d′ (mm)	A$_s$	ρ/ρ$_b$	A′$_s$	(kN/m^3) γ_C
SCCB1	33.0	256.0	42.9	2Φ18+1Φ16+1Φ14	0.511	2Φ14+1Φ18	22.80
SCCB2	31.5	255.0	43.5	4Φ20	0.746	2Φ14+1Φ20	23.03
SCCB3	35.0	254.0	45.4	4Φ22	0.91	2Φ14+1Φ25	22.60

Fig. 2. Typical test set up for loading arrangement [16]

The SCC mix was designed by the first author and the range of fresh properties is summarized in Table 2. The Flowability of SCC was determined by the slump flow test. The slump of SCC ranged between 650 and 700 mm and satisfied the recommended slump flow for SCC. The deformability of SCC and ease of flow through the restricted area without blocking were evaluated by the V-funnel and L-box tests. The flow time ranged between 3.2 and 3.9 seconds and satisfied the requirement of a maximum of 6 seconds recommended for SCC. The L-box index for SCC ranged between 0.70 and 0.77 with a mean value of 0.75 (close to the recommended range of 0.8 to 1.00 for a good SCC). With the obtained range of results in the fresh phase (Table 2), it was found that the SCC was consolidated exceptionally well under its own weight for three specimens.

Table 2. Test results of hardened and fresh concrete

| Beam No.	Slump flow dia.(mm)	L-Box h_2/h_1	Slump flow & J-Ring (mm)	V-Funnel flow time (s)
SCCB1	700 - 720	0.78	6.7	5
SCCB2	730 - 760	0.82	6.9	5
SCCB3	670 - 700	0.85	7.35	7

4.   MATERIALS PROPERTIES MODELING

4.1 Reinforced Concrete

An eight-node solid element, solid65, was used to model the concrete. The solid element has eight nodes with three degrees of freedom at each node -translations in the nodal x, y, and z directions. The element is capable of plastic deformation, cracking in three orthogonal directions, and crushing [17]. The geometry and node locations for this element type are shown in Fig. 3 (a)x.

4.2 Steel Reinforcement

A link8 element was used to model the steel reinforcement. Two nodes are required for this element. Each node has three degrees of freedom, translations in the nodal x, y, and z directions. The element is also capable of carrying plastic deformation, the geometry and node locations for this element type are shown in Fig. 3 (b).
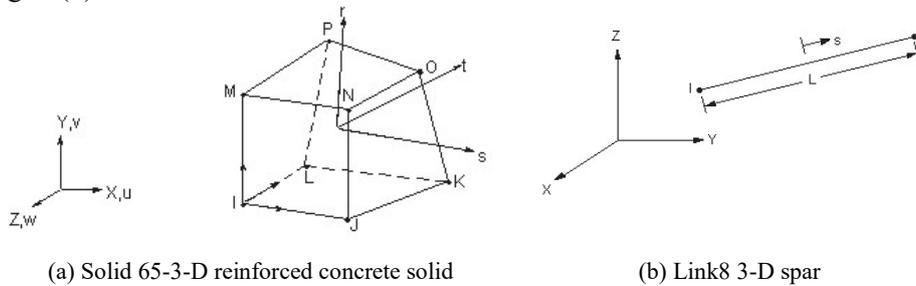
(a) Solid 65-3-D reinforced concrete solid   (b) Link8 3-D spar
Fig. 3. The geometry and node locations for elements in Ansys [15]

The development of a model for the behavior of concrete is a challenging task. Concrete is known as a quasi-brittle material and has different behavior in compression and tension. In this research, the graph of nonlinear-isotropic stress-strain of SCC is obtained from results of compression test of concrete specimens in the laboratory by helping of an embedded sensor (Fig. 4). The FE modeling of compressive concrete is performed [18] and its comparison with the experimental curve is shown in Fig. 4. A very satisfactory result is achieved.
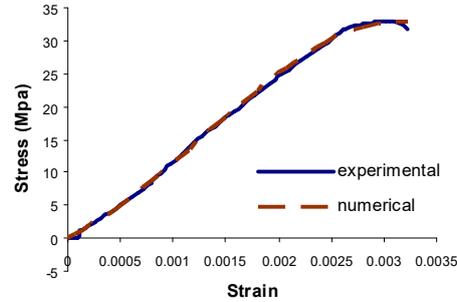
Fig. 4. Comparison of experimental and numerical analysis based on the stress-strain curve

Here, the stress-strain curve for steel reinforcement used in concrete beams was obtained from steel bars tested in tension. The curve has an initial linear elastic portion, a yield plateau (yield point beyond which the strain increases with little or no increase in stress), a strain-hardening range in which stress again increases with strain, and finally a range in which the stress drops off until fracture occurs which has been shown in Fig. 5. The Eqs. 4.1 to 4.3 used in this study are those obtained by testing the stirrup bars in tension and the stress-strain curve for steel reinforcement has the following characteristic:

1: Elastic portion; $\varepsilon_s < \varepsilon_y \qquad \Rightarrow \qquad f_s = E_s\,\varepsilon_s$ (4.1)

2: Yield plateau; $\varepsilon_y \leq \varepsilon_s \leq \varepsilon_{sh} \qquad \Rightarrow \qquad f_s = f_y$ (4.2)

3:        Strain $\varepsilon_{sh} < \varepsilon_s \leq \varepsilon_u$ (4.3)
hardening;

$$f_s = f_y + \left(f_u - f_y\right)\left[2\,\frac{\varepsilon_s - \varepsilon_{sh}}{\varepsilon_u - \varepsilon_{sh}} - \left(\frac{\varepsilon_s - \varepsilon_{sh}}{\varepsilon_u - \varepsilon_{sh}}\right)^2\right]$$

A constitutive model for the triaxial behavior of concrete [17] is used and the material properties for the concrete (ε_c', f_c') and steel reinforcement (ε_y, ε_{sh}, ε_u, f_y, f_u) are obtained and used for FE modeling.
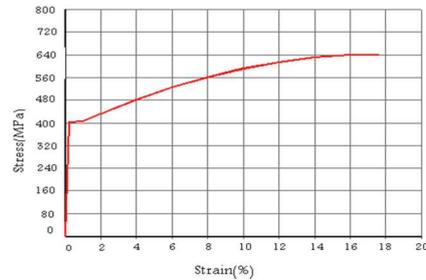
Fig. 5. Stress-strain curve of tested tensile steel

5.   FINITE ELEMENT MODELING

As an initial step, a FE analysis requires meshing of the model. In the other words, an important step in FE modeling is the selection of the mesh density. A convergence of results for steel reinforcement and concrete is obtained when an adequate number of elements are used in the model; this is practically achieved when an increase in the mesh density has a negligible effect on results. The ANSYS software [15] has been performed for nonlinear analyses and then, the steps of FE modeling are presented based on Figs 6 to 9.
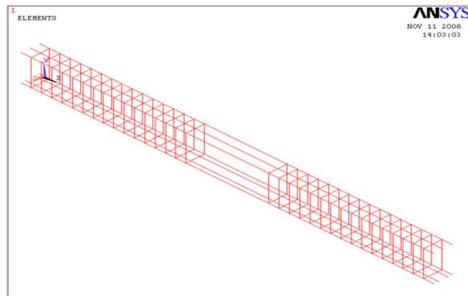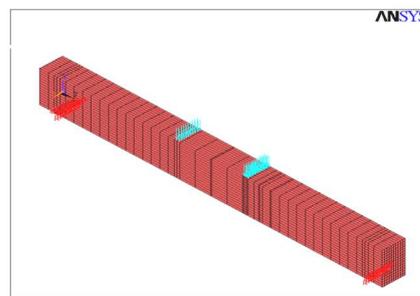

Fig. 6. The FE model of steel

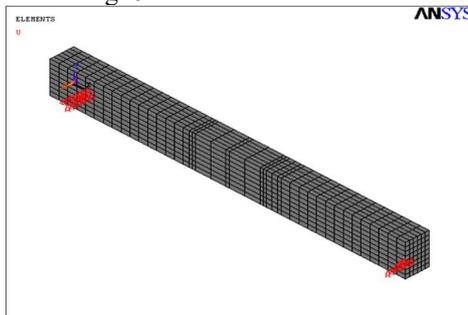Fig. 7. The FE model of concrete
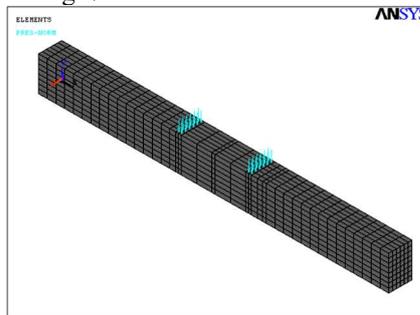

Fig. 8. Boundary conditions of FE model

Fig. 9. External loading of FE model

6. COMPARISON OF EXPERIMENTAL AND NUMERICAL RESULTS

For conventional (vibrating) concrete, the tensile diagonal stress in flexural-shear cracks has a direct relationship with the concrete tensile strength, The reinforced SCC beams were analyzed using Eq. 6.1 suggested by ACI-08 [17] for modulus of failure in conventional concrete:
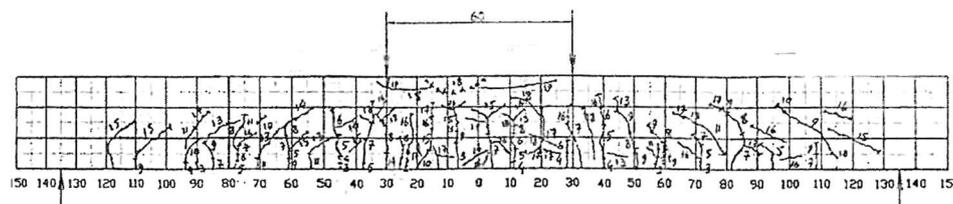
$$f_r = 0.75 \lambda \sqrt{f'_C} \quad \text{(MPa)} \quad , \lambda =/24 \tag{6.1}$$

Where, $\lambda =$ modification factor reflecting the reduced mechanical properties of lightweight concrete, all relative to normal weight concrete of the same compressive strength.
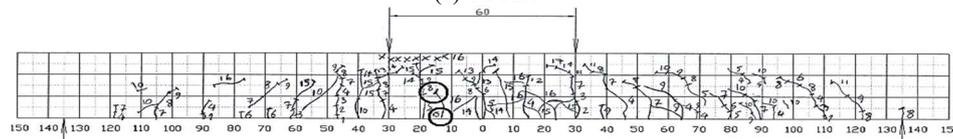
Also during the SCC beams test, the load causes to occur the first observed flexural crack/cracks were considered as (proposed) values of f_r. For each proposed value of f_r, the number, width, and depth of the initial flexural crack are taken experimentally and shown in Table 3. The types of cracks developed in tested beams are shown in Fig. 10. These two different values of f_r are used for FE shear modeling.

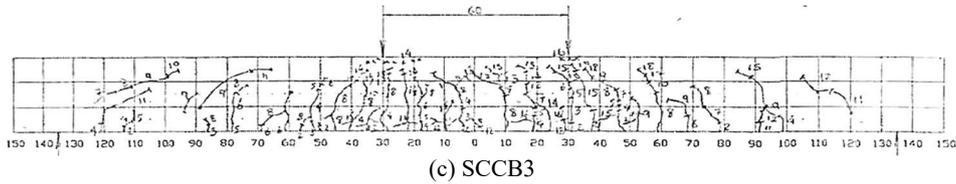Table 3. Investigation of proposed flexural strength f_r and ACI method

Beam No.	Flexural strength f_r (MPa) by Eq. (4)	Proposed flexural strength f_r (MPa)	Number of initial flexural cracks that occurred	Width of initial flexural crack (mm)	Depth of initial flexural crack (mm)
SCCB1	4.1	4.4	6	0.06	30
SCCB2	4.0	3.0	3	0.04	20
SCCB3	4.2	4.3	2	0.04	25

(a) SCCB1

(b) SCCB2

(c) SCCB3
Fig. 10. Types of cracks developed in tested beams

The load-stirrup strain curves of tested beams are plotted in Figs. 11 to13. The comparison of experimental load- stirrup strain and the FE modeling for initial flexural cracking and at the beams failure is performed and the results are given in Tables 4 and 5 respectively. As indicated, by increasing the value of f_r, the rigidity of SCC beams is slightly increased. The proposed values of f_r are higher than those obtained by ACI provisions Eq. 6.1 for conventional concrete, except for SCCB2 specimen, the initial flexural crack was not opened due to the load applied. The close observations before testing of this beam were indicated that, only one crack has occurred with a width of less than 0.01 mm. This is highlighted and shown by crack pattern "O" in Fig. (10 b). This could be due to concrete technology and not the loading cases. The crack "O" widened at the loading step of 8 (i.e., while the load reached 120 KN, this is also highlighted). In other words, as shown in Table 3, due to the applied load of step 1 (i.e., the load was 10 KN) on SCCB2 beam, the first flexural crack was occurred with a width of 0.04 mm.

The results of FE analysis with proposed and ACI values of f_r is indicated that a very good agreement is available with that of the experimental result. Meanwhile, the results of Load-shear strain curves are presented based on Figs. 11 to 13.
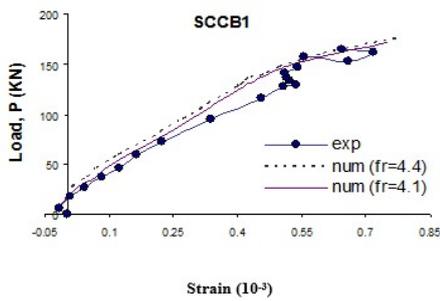

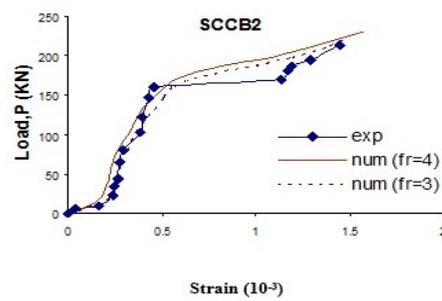Fig. 11. Load-shear strain of No. 2 stirrup for different values of f_r

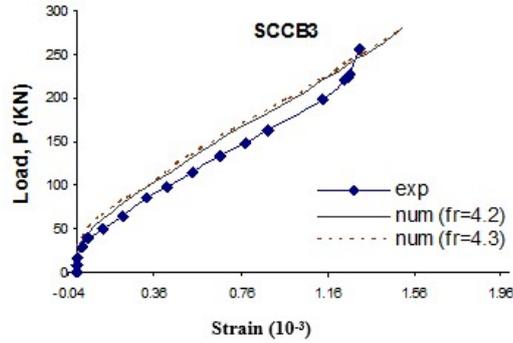Fig. 12. Load-shear strain of No. 2 stirrup for different values of f_r

Fig. 13. Load-shear strain of No. 2 stirrup for different values of f_r

Table 4. Comparison of the load-shear strain by FE analysis and experimental results for different f_r values at flexural cracking of beams

Beam No.	f_r (MPa)		Numerical analysis results		Experimental results		Error	
			p_{cr} (kN)	$\varepsilon_{s_{cr}}$ (10^{-3})	p_{cr} (kN)	$\varepsilon_{s_{cr}}$ (10^{-3})	p_{cr}	$\varepsilon_{s_{cr}}$
SCCB1	proposed	4.4	19.1	0.008	17.33	0.009	0.09	0.11
	Eq. (4)	4.1	18.5	0.0083			0.06	0.08
SCCB2	proposed	3.0	10.5	0.0034	10	0.0036	0.05	0.06
	Eq. (4)	4.0	12	0.0029			0.16	0.19
SCCB3	proposed	4.3	17.3	0.0037	16	0.004	0.08	0.08
	Eq. (4)	4.2	17	0.0038			0.06	0.05

Table 5. Comparison of the load-shear strain of FE and experimental results for different f_r values at beams failure

Beam No.	f_r (MPa)		Numerical analysis results		Experimental results		Error	
			p_u (kN)	$\varepsilon_{s_{cr}}$ (10^{-3})	p_u (kN)	$\varepsilon_{s_{cr}}$ (10^{-3})	p_u	ε_{s_u}
SCCB1	proposed	4.4	180	0.79	164.66	0.643	0.09	0.18
	Eq. (4)	4.1	172	0.75			0.04	0.14
SCCB2	proposed	3.0	220	1.51	214.66	1.453	0.03	0.04
	Eq. (4)	4.0	231	1.60			0.07	0.09
SCCB3	proposed	4.3	280	1.52	256	1.307	0.09	0.14
	Eq. (4)	4.2	278	1.50			0.08	0.13

7. SHEAR STRESS CALCULATION AND WIDTH OF FLEXURAL-SHEAR CRACKS

The comparison of FE modeling and the experimental shear stress values are performed and the curves are shown in Figs. 14 to 16.
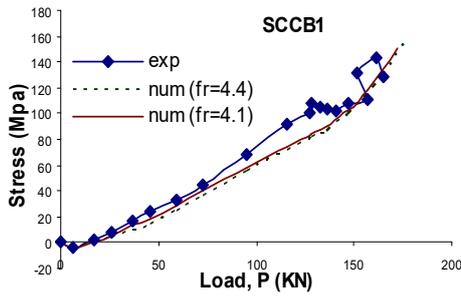

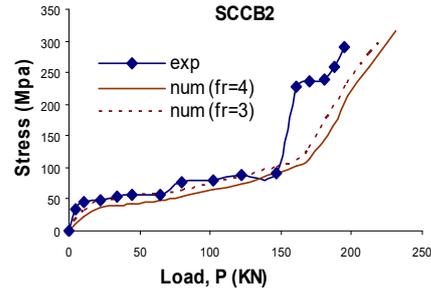Fig. 14. Load-shear stress of No. 2 stirrup for different values of f_r

Fig. 15. Load-shear stress of No. 2 stirrup for different values of f_r
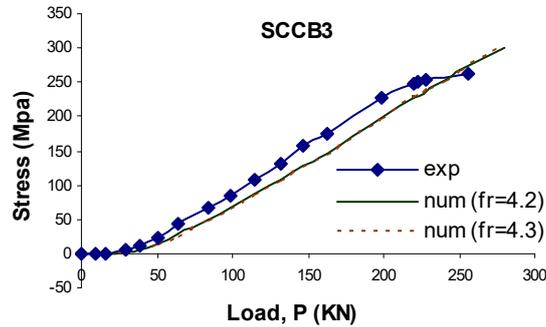

Fig. 16. Load-shear stress of No. 2 stirrup for different values of f_r

The shear calculations for SCC tested beams are performed based on Eqs. 7.1 and 7.2 given for conventional concrete and also strength due to stirrups are found and the results are shown in Tables 6 and 7 respectively.

$$\vartheta_c = \lambda \sqrt{f'_C} / 6 \ \ (\text{MPa}) \tag{7.1}$$

$$V_c = \vartheta_c \, b_w d \ \ (\text{kN}), \ \ V_s = V_n - V_c \ \ (\text{kN}) \tag{7.2}$$

Where, ϑ_c = The concrete shear strength, V_n = The total shear force.

Table 6. Comparison between concrete shear strength of ACI and proposed value

Beam No.	ϑ_c (ACI) (MPa)	ϑ_c (proposed) (MPa)	Error	Width of first shear crack (mm)
SCCB1	0.9	0.65	0.27	0.05
SCCB2	0.89	0.69	0.22	0.04
SCCB3	0.92	0.70	0.24	0.02

Table 7. Comparison between load-stirrup stress of FE modeling and experimental results for different f_r values at the failure of beam

Beam No.	f_r (MPa)		Numerical analysis Results ϑ_s (MPa)	Experimental Results ϑ_s (MPa)	Error
SCCB1	Proposed	4.4	158	129	0.18
	Eq. (4)	4.1	150		0.14
SCCB2	Proposed	3.0	302	290.6	0.04
	Eq. (4)	4	320		0.09
SCCB3	Proposed	4.3	304	262	0.14
	Eq. (4)	4.2	300		0.13

8. CONCLUSION

The current study presents results of the FE analysis and experimental work of three reinforced SCC beams in shear taking into account, the flexural tensile strength f_r of concrete. The load-stirrup strain and load-stirrup stress curves for different values of f_r obtained by the FE model and the ACI and theproposed values were compared and it was almost concluded that, the obtained curves are coinciding with each other up to the load causes the occurrence of flexural-shear cracks. They are then separated from each other but never the percentage of error has been more than 15%.

The proposed values of f_r are higher than those obtained by ACI provisions for conventional concrete, for SCCB1, SCCB3, and smaller for SCCB2 beams (i.e., f_r =0.78 $\lambda \sqrt{f_C'}$ and f_r =0.56 $\lambda \sqrt{f_C'}$ respectively). By increasing the value of f_r, the rigidity of SCC beams is slightly increased.

Comparison of FE analysis and experimental results of stirrup-strain at flexural cracking $\varepsilon_{s_{cr}}$ are very low and this is an indication of the superiority of this type of concrete (non-vibrating concrete) in resisting shear force before crack. At the occurrence of flexural-shear cracks, very narrow cracks are opened (i.e., their width was ranging from 0.05, 0.04 and 0.02 mm for SCCB1 to SCCB3). In other

words, a lower value of $\vartheta_c \cong \lambda \sqrt{f'_C} /8$ is obtained for concrete participation while considering the SCC in shear resistance calculations. Although the stirrups provided in the beams were almost half the amount required by ACI provision for conventional (vibrating concrete) concrete, nevertheless, at ultimate failure the values of stirrup stress, ϑ_s was never yielded. This is again an indication of the superiority of SCC to transfer the load to stirrups, slowly and safely. The percentage of error for numerical and experimental values of ϑ_s is varied from 4% to 18%, which is indicated that a reasonably good accuracy is achieved.

REFERENCES

1. Okamura, H 1997. Self-Compacting High-Performance Concrete. *Concrete International* **19 (7)**, 50–54.
2. Poppe, AM and De Schutter, G 2001. Influence of the Nature and the Grading Curve of the Powder on the Rheology of Self-Compacting Concrete. Proceedings of the Fifth CANMET/ACI *International Conference Recent Advances in Concrete Technology*, Singapore, 399–414.
3. Khalily, M Saberi, V Saberi, H Mansouri, V Sadeghi, A and Pachideh, G 2021. An Experimental Study on the Effect of High Temperatures on Performance of the Plastic Lightweight Concrete Containing Steel, Polypropylene and Glass Fibers. *Journal of Structural and Construction Engineering*.
4. Khatab, TAM Ashour, FA Sheehan, T and Lam, D 2017. Experimental investigation on continuous reinforced SCC deep beams and Comparisons with Code provisions and models. *Eng. Struct.* **131**, 264–274.
5. Hossain, K. A Lachemi, M and Hassan, A 2008. Behaviour of Full-scale Self-Consolidating Concrete Beams in Shear. *Cement and Concrete Composites* **30**, 588–596.
6. Fritih, Y et al. 2013. Flexural and shear behavior of steel fiber reinforced SCC beams. *KSCE J Civ Eng* **17**, 1383–1393.
7. Ahmed, S Umer, A and Masood, A 2016. Properties of Normal, Self-Compacting Concrete and Glass Fibre-Reinforced Self-Compacting Concrete: An Experimental Study. *11th International Symposium on Plasticity and Impact Mechanics*, 807–813.
8. Lif, SL Shahiron, S Mohamad, SS and Nurul, IIR, H 2016. A Preliminary Study on Chemical and Physical Properties of Coconut Shell Powder As A Filler in Concrete. *Materials Science and Engineering* **160**, 1–7.

9. Tahir, M 2018. Str*uctural performance of precast self-compacting concrete beam consisting banana skin powder and coir fibre under flexural load*, PhD thesis. Johar: Universiti Tun Hussein Onn Malaysia.
10. Akinpelu, M and Adedeji, A 2018. Structural Response of Reinforced Self-Compacting Concrete Deep Beam Using Finite Element Method. *Journal of Soft Computing in Civil Engineering* **2(1)**, 36-61.
11. Aydin, AC and Bayrak B 2019. The torsional behavior of reinforced self-compacting concrete beams. *Advances in Concrete Construction* **8(3)**, 187-198.
12. Akinpelu, MA Odeyemi, SO Olafusi, OS and Muhammed, FZ 2019. Evaluation of splitting tensile and compressive strength relationship of self-compacting concrete. *Journal of King Saud University - Engineering Sciences* **31(1)**, 19-25.
13. Jain, A Gupta, R and Chaudhary, S 2020. Sustainable development of self-compacting concrete by using granite waste and fly ash. *Construction and Building Materials* **262**.
14. Hussein, LF Khattab, MM Farman, MS 2021. The torsional behavior of reinforced self-compacting concrete beams, Experimental and finite element studies on the behavior of hybrid reinforced concrete beams. *Case Studies in Construction Materials* **15**.
15. ANSYS, ANSYS User's Manual, Version 9.
16. Diba, SM 2007. *Behavior of Beams with Self-Compacting Concrete under Flexure*, Master thesis. Tehran: Iran University of Science and Technology.
17. ACI 440.2R-08 2008. *Guide for the Design and Construction of Externally Bonded FRP Systems for Strengthening Concrete Structures*.
18. William, KJ and Warnke, ED 1975. Constitutive Model for the Triaxial Behaviour of Concrete, P*roceedings of the International Association for Bridge and Structural Engineering* **19**.